

EULERIAN MODEL FOR DISSOLUTION AND DISPERSION OF PARTICLES ENTERING A LIQUID

James W. HOLBEACH and Malcolm R. DAVIDSON

Dept. Chemical and Biomolecular Engineering, University of Melbourne, Parkville, Victoria 3010, AUSTRALIA

ABSTRACT

The dispersion of a cloud of dissolving particles entering an initially quiescent liquid is modelled numerically using a transient Eulerian-Eulerian finite volume method. A simplified treatment of dissolution is presented in which the dissolution rate is determined by a specified change in particle diameter with time. The effect of dissolution time and density ratio in the predicted dispersion is discussed. For particles more dense than the liquid, dissolution was found to have little effect on the general shape and dispersive evolution of the particle plume regardless of density ratio or dissolution time. However it was found to reduce penetration depth, the effect being greater for increased particle density. A plume of neutrally buoyant particles is predicted to form a more complex shape with an expected lower penetration depth than for more dense solids. Dissolution is found to have little effect on the spreading of a neutrally buoyant plume.

NOMENCLATURE

ΔC	concentration difference
d	particle diameter
\mathbf{F}	momentum transfer source term
\mathbf{g}	gravity
h_p	plume height
k_m	mass transfer coefficient
n	number density
n_l	limiting number density
\dot{m}	mass flowrate
P	pressure
t	time
t_d	dissolution time
t_p	pulse length
\mathbf{U}	velocity
v_i	inlet velocity
\bar{v}	weighted average velocity
w_p	plume width
x_c	x ordinate of centroid position
y_c	y ordinate of centroid position
α	volume fraction
μ	dynamic viscosity
ρ	density
τ	stress term
Subscripts	
0	initial conditions
s	solid phase
l	liquid phase

INTRODUCTION

Dissolution and dispersion of solids entering a liquid is important in many different areas. Common examples are salt dissolving in water or, in an alloying process, molybdenum particles (Molybdenic Oxide) dissolving in molten steel. Other examples involving addition to metallurgical melts include: pelletized directly reduced iron (DRI) added to an electric arc furnace (Brown, 1979), or the addition of alloying materials such as nickel or aluminium.

The dispersion of inert solids entering liquids has been successfully and accurately modelled in the past. Suitable techniques were developed in the context of Nuclear reactor safety (Gilbertson et al., 1992, Fletcher et al., 1996). These were extended by Smith et al. (1997) who developed a computational model for the dispersion of a solids stream entering an initially quiescent liquid. In subsequent experimental work (Smith, 2000) showed that computational simulations predict well the dispersion of inert solids. Tanaka et al. (1993) have also obtained good agreement between predicted and measured trajectories of individual particles, especially in quiescent systems. Guthrie et al. (1976) also examined the penetration of single spherical particles in metallurgical baths, and showed that submerged melting of positively buoyant solids does not occur regardless of entry parameters, which is important in alloying processes.

Dissolution is a well understood process. Numerical and experimental models have been developed in various contexts and for particular systems. Wright and Baldock (1988), for example, examined the dissolution of graphite into steel melts. This process is of particular importance when carbon saturation of the iron is to be achieved. They used mathematical models of dissolution to support their experimental findings. Nickel may be alloyed with zinc in galvanizing of steel. Langberg and Nilmani (1996) developed a model of the dissolution of nickel in zinc which was based upon work by Apelian et al. (1980). This model allowed an analytical rather than a numerical solution. Hu and Argyropoulos (1997) modelled the dissolution of a cylindrical rod in high and low temperature systems, and obtained good agreement with experimental results. They discussed the exothermic heat of mixing and related modifications to the heat and mass transfer equations.

While much work has focused upon the individual effects of dissolution and dispersion, the effect of the two processes in combination has received little attention

within the context of particulate solids addition to liquids. The inclusion of dissolution alters the dispersion of solids in various ways. A changing particle diameter will alter the drag force experienced and so can have a significant effect upon the penetration and dispersion. Mass transfer may lead to changes in the liquid density, momentum transfer from the solid to the liquid phase, or liquid viscosity changes due to additional components being dissolved into the liquid, all of which may be important. For example, in the case of salt dissolution into water, density variations normally result in natural convection (Hameed, 1995).

Recently, the authors (Holbeach and Davidson, 2004) extended the computational dispersion model of Smith (2000) to include dissolution of solids under isothermal conditions. Thus heat transfer effects associated with dissolution, which can affect the flow field (Hu and Argyropoulos, 1997), were ignored, and the interplay between particle dispersion and reducing particle size was explored without the complicating effects of heat transfer. Under isothermal conditions the problem presents itself as an examination of the dispersion of falling particles whose diameter changes with time. The aim of the present paper is to summarise the authors' model and to examine how particle density in association with dissolution time affects the predicted dispersion and penetration of a dissolving plume of particles.

FORMULATION

Problem Definition

The present work examines the penetration of a short pulse of dissolving spherical solid particles (of initial diameter 6.25mm) dropped into an initially quiescent fluid. The pulse or cloud of particles dissolves and disperses as it descends (Figure 1). The computational simulation is based on the validated model of Smith (2000) for non-dissolving particles.

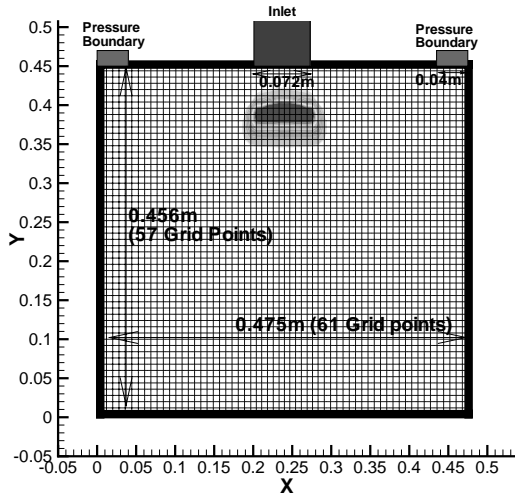


Figure 1: A schematic of the computational domain. Slip walls either side of the inlet represent the free surface, and pressure boundaries are placed in either corner to allow displaced fluid to exit. All other walls are non slip.

MODEL FORMULATION

Transport Equations

The governing transport equations for the present case are those for a multiphase Eulerian, two dimensional, laminar system. We let the subscripts 's' and 'l' denote the solid and liquid phases respectively. The continuity equation then takes the form:

Liquid Phase:

$$\frac{\partial}{\partial t}(\rho_l \alpha_l) + \nabla \cdot (\alpha_l \rho_l \mathbf{U}_l) = \dot{m}_{ls} \quad (1)$$

Solid Phase

$$\frac{\partial}{\partial t}(\rho_s \alpha_s) + \nabla \cdot (\alpha_s \rho_s \mathbf{U}_s) = -\dot{m}_{ls} \quad (2)$$

where \mathbf{U} denotes the velocity, while ρ , α and t , denote the density, volume fraction and time respectively. \dot{m}_{ls} represents the mass flow rate from the solid phase into the liquid per unit volume. The momentum equations can be written:

Liquid Phase:

$$\frac{\partial}{\partial t}(\alpha_l \rho_l \mathbf{U}_l) + \nabla \cdot (\alpha_l \rho_l \mathbf{U}_l \mathbf{U}_l) = \nabla \cdot (\alpha_l \boldsymbol{\tau}_l) - \alpha_l \nabla P + \alpha_l \rho_l \mathbf{g} - \mathbf{F}_s^D - \mathbf{F}_s^{MT} - \mathbf{F}_s^L - \mathbf{F}_s^{AM} \quad (3)$$

Solid Phase:

$$\frac{\partial}{\partial t}(\alpha_s \rho_s \mathbf{U}_s) + \nabla \cdot (\alpha_s \rho_s \mathbf{U}_s \mathbf{U}_s) = -\alpha_s \nabla P + \alpha_s \rho_s \mathbf{g} + \mathbf{F}_s^D + \mathbf{F}_s^{MT} + \mathbf{F}_s^L + \mathbf{F}_s^{AM} + \mathbf{F}_s^{SP} \quad (4)$$

Here P , and \mathbf{g} represent the pressure and gravity, while $\boldsymbol{\tau}_l$ is the liquid viscous stress term. The terms \mathbf{F}_s^D , \mathbf{F}_s^{MT} , \mathbf{F}_s^L , and \mathbf{F}_s^{AM} refer to interfacial momentum transfer due to drag, mass transfer, lift and added mass, respectively. In the solid phase the pressure is assumed to be the same as that in the liquid phase. However, an additional term \mathbf{F}_s^{SP} denoting the solids pressure, is included to allow for particle-particle interactions (Syamlal, 1985, 1988), preventing particle volume fractions from rising to unrealistic values. A more complete description of the terms here can be found in Holbeach and Davidson (2004).

A second order upwind advection differencing scheme, with Van-Leer flux limiting (Van-Leer, 1974) is used for all transported variables as this helps reduce numerical smearing at the phase boundaries. Grid independence is achieved via a slightly non uniform (61×57) grid with an approximate grid spacing of 0.8mm (occasionally a 61×157 with the same grid spacing). The coupled equations above are solved using the fluid flow package CFX 4.4 (AEA Technology, 1997). Time step independence is achieved using fixed time stepping of 2ms, while convergence is considered to have occurred when all normalised residuals are less than 2×10^{-5} .

Dissolution

The particles are assumed to dissolve via a simple dissolution model, whereby their diameter (d) decreases linearly with time according to Equation 5 (See Holbeach and Davidson (2004) for details).

$$d(t) = d_0 \left(1 - \frac{t}{t_d} \right) \text{ for } t \leq t_d \quad (5)$$

$$\text{where } t_d = \frac{\rho_s d_0}{k_m \Delta C} \quad (6)$$

Here d_0 , k_m , and ΔC refer to the initial particle diameter, mass transfer coefficient, and concentration difference between the particle interface and the fluid bulk, respectively. The parameter t_d is the dissolution time (i.e. the time it takes the particle to dissolve completely). The parameters ΔC , and k_m are assumed to be constant. While the concentration difference is unlikely to change significantly in dilute systems, k_m will depend upon both the particle diameter and slip velocity. However, for the bulk of the particles dissolution history, other work (Langberg et al., 1996) shows k_m to be relatively constant for a given slip velocity.

By considering a short pulse (relative to the particulate dissolution time), assumptions may be made regarding the dissolution of **all particles** in the system. It is assumed that:

- The pulse is short enough ($t_p=0.2s$) that all particles may be regarded as having been exposed to the liquid for the same length of time. This allows us to ignore the fact that solids entering first start dissolving before those which enter later. In the simulation we assume that dissolution begins once all the particles have entered.
- All particles experience the same (constant) slip velocity, in regard to dissolution. This assumption allows us to assume that all particles have the same (constant) mass transfer coefficient, allowing Equation 5 to be used for **all** particles. Note that the constant slip velocity assumption only applies to the formulation of Equation 5. Slip velocities actually calculated within the two-fluid calculations will vary in time and position, in general. However, this assumption is reasonable as all particles fall at approximately the same rate through what can be regarded as an essentially stationary liquid.
- It is assumed that the influence of the dissolution process upon the physical properties of the liquid phase is negligible.

Given the above assumptions, the history of individual particles is then irrelevant and all particles may be considered to dissolve at exactly the same rate, and hence have the same radius at any time (given by Equation 5). Momentum, mass transfer and transient drag considerations associated with the dissolution process, are discussed by Holbeach and Davidson (2004).

Base Parameters

Base simulation parameters (no dissolution) shown in Table 1 were taken from Smith (2000). In the present case we will use the same parameter set, modifying only three of the variables, the pulse length, dissolution time and solid density. Making this slight extrapolation from previously validated work gives confidence that the present results are reasonable.

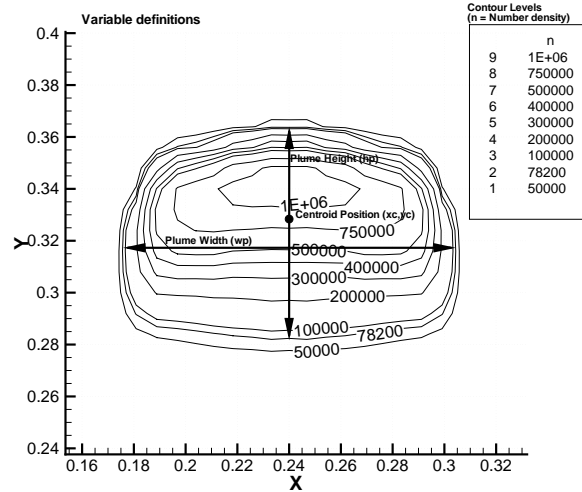


Figure 2: A sample plot showing the plume shape variables used in the analysis of the dissolution process. The contours show number density of solids within the liquid. The plume centroid position, width and height are shown.

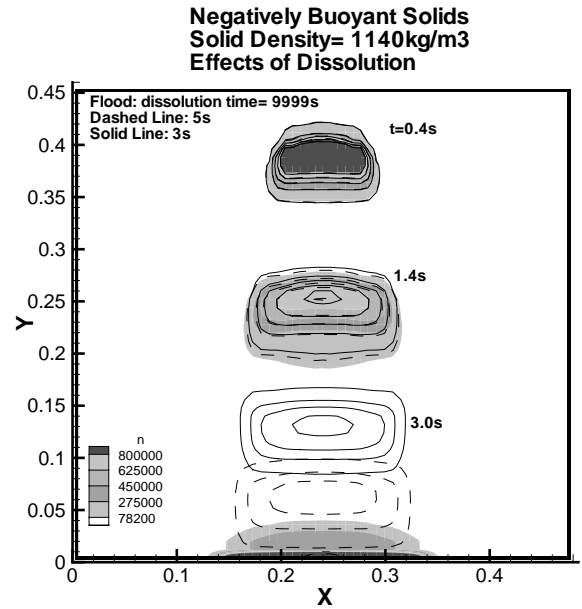


Figure 3: The dispersion of a plume of solids (where $\rho_s/\rho_l=1.14$) descending through an initially quiescent bath, with dissolution (Solid Lines $t_d=3s$, dashed lines $t_d=5s$) and without dissolution (Flood Contour)

Parameter	Variable	Value	Units
Solid Density	ρ_s	1140	kgm^{-3}
Liquid Density	ρ_l	1000	kgm^{-3}
Liquid Viscosity	μ_l	0.001	$\text{kgm}^{-1}\text{s}^{-1}$
Initial Particle Diam.	d_0	0.00625	m
Inlet Velocity	v_i	0.80	ms^{-1}
Inlet Volume Fraction	α_s	0.039	[-]
Pulse Length	t_p	∞	s
Dissolution time	t_d	∞	s

Table 1: Base Case Simulation Parameters. No dissolution.

DISCUSSION OF RESULTS

As the particles dissolve, number density is used to track the particles dispersion as it will not be affected by particle size, only the number of particles within a given volume.

$$n = \frac{\text{Number of particles}}{\text{Unit volume}} \quad (7)$$

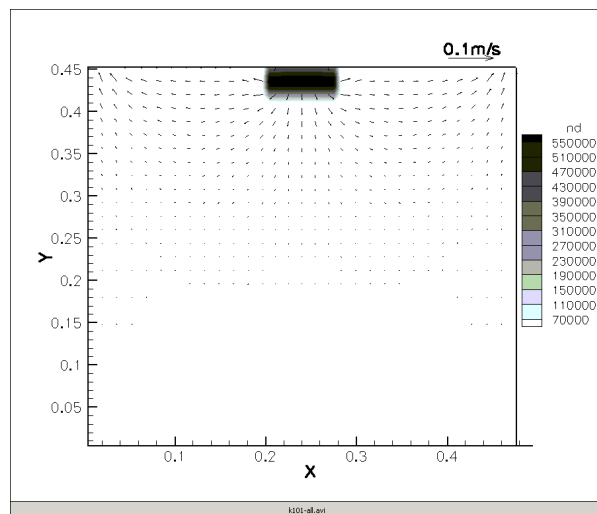
$$= \frac{6\alpha_s}{\pi d^3}$$

However, the number density is a continuous variable in our Eulerian model, and thus we need to define a limiting number density (n_l) to determine the edge of the solid plume (i.e. for number densities below the n_l value we consider no/negligible solids to be present for the purposes of visualization). The value for n_l is chosen arbitrarily to be $n_l = 78,200$ corresponding approximately to a volume-fraction of 1% with the initial particle size of 6.25mm . The plume width (w_p) and plume height (h_p) correspond to the maximum horizontal and vertical extent of the limiting number density contour as indicated in Figure 2. The centroid position (x_c, y_c) is an average location, weighted by n .

Solids Denser than Liquid

In earlier work (Holbeach & Davidson, 2004), the effect of dissolution upon the diffusion of solids was examined by varying the time taken for the solids to dissolve completely (i.e. varying the t_d parameter) in systems where $\rho_s/\rho_l = 1.14$. We now examine to what extent the density of the solid phase affects the dispersion of solids in our simplified dissolution model.

Figure 3 shows the dispersion of a plume of solids ($\rho_s/\rho_l = 1.140$) for differing dissolution rates. The $t_d = 9999\text{s}$ case is used to represent the case of no dissolution. As the solid particles descend through the domain, their plume spreads both vertically and horizontally while retaining the broad features of its primary shape (a rectangle with rounded corners).



Animation 1: An animation over 8 seconds is presented, showing the dispersion of a short pulse ($t_p = 0.2\text{s}$) of dissolving solids ($\rho_s = 1010\text{kg/m}^3$, $t_d = 8.0\text{s}$)

This is also demonstrated in the attached animation file (Animation 1). This animation shows the dispersion of a plume of a solids ($\rho_s/\rho_l = 1.01$) as it dissolves over 8 seconds. Although the density ratio in this case is significantly lower than that examined previously, the same effects are seen. The actual shape of the descending plume does not change much during its decent. However, it is clear that for this reduced density ratio, the dispersion is affected more significantly by the fluid flow field. The sides of the plume are seen to be more swept back, due to a lower terminal velocity allowing the liquid flow field to affect the plume dispersion at early times.

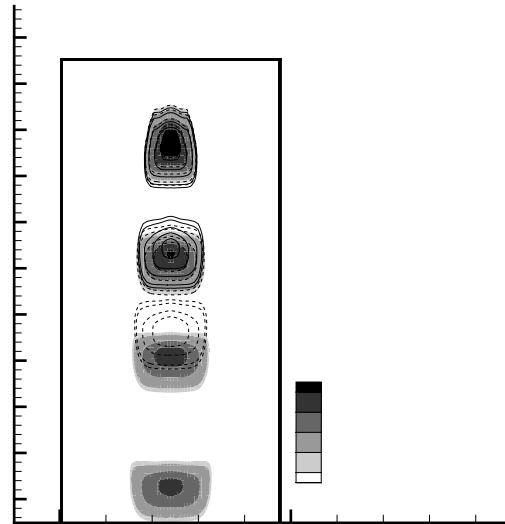


Figure 4: The dispersion of a plume of solids (where $\rho_s/\rho_l = 3.0$) descending through an initially quiescent bath, with dissolution, Solid Lines $t_d = 0.69\text{s}$, dashed lines $t_d = 1.145\text{s}$ and Flood Contour $t_d = 2.0\text{s}$.

In contrast, the dispersion of a denser plume of solids ($\rho_s/\rho_l = 3.0$ - Figure 4) is more elongated than in the $\rho_s/\rho_l = 1.14$ case (Figure 3). This occurs because the entry velocity of the solids, in the higher density case, is closer to their initial terminal falling velocity, thus the vertical compression of the plume, due to the velocity difference between the front and rear of the plume, is less.

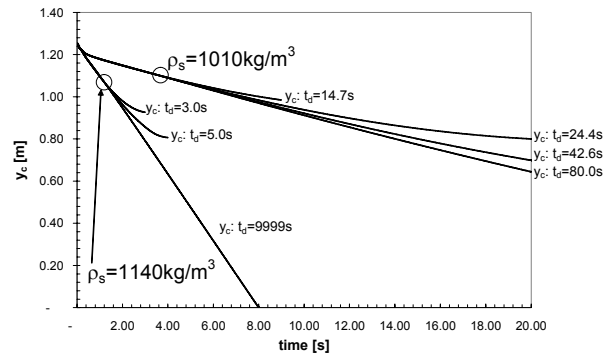


Figure 5: The position of the centroid in the vertical direction) of a plume of solids ($\rho_s/\rho_l = 1.01$ and 1.14) as it descends through the domain over time, is presented

The general shape of the plume for a given $\rho_s/\rho_l > 1$ remains relatively similar at all times, regardless of the dissolution parameter (see Figures 3 and 4 and Animation 1). This is primarily caused by liquid velocity being smaller in magnitude than the corresponding solid velocity, for most times, dissolution rates and density ratios as is discussed below. Thus the fluid flow field has little effect upon the plume, until the particle size is very small and the solid velocity is close to the liquid velocity (as discussed below).

In all these cases dissolution is seen to hinder penetration depth regardless of density ratio. Figure 5 shows the y-centroid position as a function of time for two different density ratios. It is clear that increasing the rate of dissolution limits penetration depth, as found in previous work (Holbeach and Davidson, 2004). This result is found to extend to all cases involving negatively buoyant solids, but was enhanced by increased density ratios. That is, the proportional reduction in penetration depth due to dissolution was greater for denser solids.

In the case of no dissolution, after an initial deceleration, the position of the centroid decreases approximately linearly with time (Figure 5) corresponding to a rapid approach to terminal velocity for the solid plume. As the solid particles move through the fluid, they induce a fluid velocity field. However, this liquid velocity field is relatively low in magnitude compared to the terminal falling velocity of the solids for most times and dissolution rates. Therefore, any change in the liquid velocity will make little difference to the dispersion of the solid plume. Essentially the solids fall through a fluid which remains almost quiescent, which is why the plume shape remains fairly consistent throughout its descent. With no dissolution, the solids slow rapidly to a velocity close to their terminal velocity. This is achieved more rapidly for low density solids, as they do not have as much inertia upon entering the domain. With no dissolution the particle diameter remains constant as does the terminal velocity throughout descent of the plume. When dissolution is included, however, the particle radius decreases, and the terminal velocity also decreases. This explains the reduction of penetration depth by dissolution.

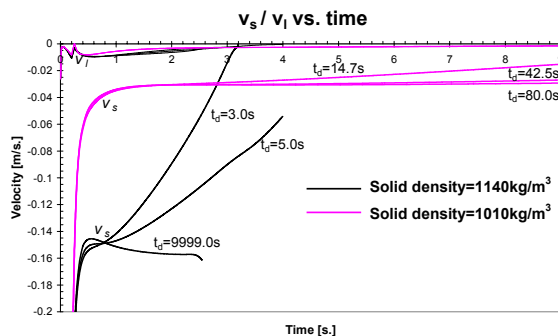


Figure 6: The weighted average solid and liquid velocities are presented for different dissolution rates. The pink line represents results for a solid density of 1010kg/m^3 while the black line presents the 1140kg/m^3 solids.

While the flow field is enhanced by momentum transfer from the solid to the liquid phase during the plumes

descent, most of the momentum transfer to the liquid phase occurs during the initial entry period. As noted in Holbeach and Davidson (2004), the key feature of the liquid flow field is the formation of two recirculations either side of the centreline, behind the trailing edges of the plume (see Animation 1). In all negatively buoyant cases, this recirculation descends through the domain behind the main solid plume, and thus has only a slight effect upon it, enhancing horizontal dispersion a little. Horizontal and vertical dispersion of the plume are not greatly effected by the inclusion of dissolution in the simulation. Some slight dependence between the two plume shape variables (w_p and h_p) and the dissolution parameter (t_d) was observed in Holbeach and Davidson (2004), however this dependence was found to be small, and not significantly related to density.

Neutrally Buoyant Solids

In contrast to the negatively buoyant case, the neutrally buoyant plume changes shape significantly over time as illustrated in Figure 7. Major features of the plume which develop are the "Lobes", "Tail" and "Head", as shown in Figure 7. The general properties of the plumes evolution can be broken up into 3 sections.

- Initial entry and lobe formation
- Head formation
- Tail formation and head evolution.

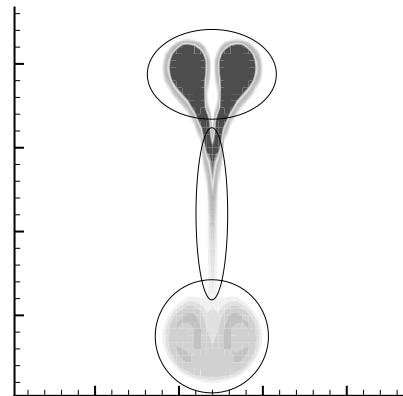


Figure 7: The dispersion of a neutrally buoyant plume of solids shows features which are given the names shown.

The formation of the lobes occurs over the first 10 seconds. The formation of the head of the plume occurs between 10 and 20 seconds after the particles entry, while the formation of the tail and evolution of the head continues from 15 seconds onwards. A more detailed explanation of these stages of the plumes evolution can be found in Holbeach and Davidson (2004).

Figure 8 shows the effect of dissolution on the pattern of dispersion of neutrally buoyant solids. In contrast to the negatively buoyant case, dissolution is seen to have a minimal effect on the plume dispersion. As discussed earlier, the penetration depth of the plume is controlled by the terminal falling velocity of the particles. However, the downwards velocity of neutrally buoyant particles is less than for negatively buoyant ones, and approaches their terminal velocity which is zero at all times, for all particle diameters. In that case the drag force becomes zero. This explains why dissolution has little effect on dispersion of the neutrally buoyant plume.

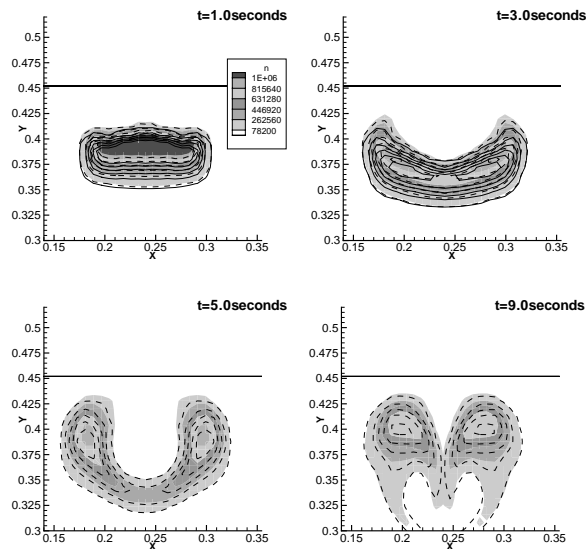


Figure 8: Number density contours for neutrally buoyant solids dispersing and dissolving. Flood, dashed, and solid line contours refer to cases of $t_d=9999$, 10 and 3s respectively

CONCLUSION

For negatively buoyant dissolving particles ($\rho_s / \rho_l > 1$), a "pulse" of entering solids is predicted to form a plume which retains a regular shape as it descends through the liquid. The plume is seen to disperse slowly in both the vertical and horizontal direction. Solid density affects the influence of dissolution on the vertical penetration of the solid plume in the domain. Overall, however, the density of the solids was found to have little significant effect upon the way in which dissolution alters the dispersive evolution of a falling plume of solids. When neutrally buoyant particles are considered, the solids plume is predicted to form a more complex shape in which most of the particles are retained in a pair of stationary lobes connected by a tail to an advancing pair of vortices of much lower particulate concentration. Penetration depth is lower than for more dense solids, as expected. The bulk of the particles rapidly cease their downwards motion (zero terminal velocity) after which the plume continues to change shape. Dissolution, in the case of neutrally buoyant solids, is found to have little effect on the dispersion of the plume. This occurs because the spreading mechanism involves the drag force which is small when the particle and liquid velocities are small.

ACKNOWLEDGEMENTS

This work has been made possible with the help of a G.K. Williams Co-operative Research Center (G.K.W C.R.C) Studentship. Special thanks should also go to David Fletcher of the University of Sydney, who helped in the development of specific user routines for drag within CFX.

REFERENCES

AEA TECHNOLOGY (1997), CFX-4.4: Solver User Guide, Harwell Laboratory, Oxfordshire.

APELIAN, D., O'MALLEY, R., DREMANN, C. (1980), "Injection of Non-Buoyant Particles", *Proc. SCANINJECT II*, Mefos and Jernkontoret, Lulea Sweden, 7:1-7:33.

BROWN J. W., and REDDY, R.L. (1979), "Electric Arc Furnace Steelmaking with Sponge Iron", *Ironmaking and Steelmaking*, 24-31.

FLETCHER D. F. and WITT P. J. (1996), "Numerical Studies of Multiphase Mixing with Application to some Small-Scale Experiments", *Nuclear Eng. and Des.*, **166**, 135-145.

GILBERTSON, M. A. ET AL. (1992), "Isothermal Coarse Mixing: Experimental and CFD Modelling", *Third U.K. National Conf. Incorporating 1st European Conf. on Thermal Sciences*, Birmingham 16-18 September, **1**, 547-556.

GUTHRIE, R.I.L., GOURTZOYANNIS, L., and HENEIN, H. (1976), "An Experimental and Mathematical Evaluation of Shooting Methods for Projecting Buoyant Alloy Additions into Liquid Steel Baths", *Can. Met. Quarterly*, **15**, 145-153.

HAMEED, M.S., and BATA, F.Y. (1995), "Experimental and Mathematical Studies of Natural Convection for Solid Salt Dissolution in Water", *Can. J. Chem. Eng.*, **73**, 924-930.

HOLBEACH, J. W. and DAVIDSON, M. R. (2004), "Modelling the dispersion of dissolving spherical particles." *Prog. CFD J.*, In Press.

HU, H. and ARGYROPOULOS, S. A., (1997), "Mathematical Simulation and Experimental Verification of Melting from the Coupled Effect of Natural Convection and Exothermic Heat of Mixing", *Met. Trans. B*, **28B**, 135-148.

LANGBERG, D.E., and NILMANI, M. (1996), "The production of Nickel-Zinc Alloys by Powder Injection", *Met. Trans B*, **27B**, 780-787.

SMITH, K. M., DAVIDSON, M. R., and FLETCHER, D. F. (1997), "Dispersion of a Solids stream falling into a Stationary Liquid", *Int. Conf. CFD in Min. Met. Proc. And Power Gen*, Melbourne 3-4 July, 133-140.

SMITH, K. M. (2000), "Dispersion of solids dropped as a continuous stream into a liquid", *PhD Thesis*, The University of Melbourne, Australia.

SYAMLAL, M and GIDASPOW, D. (1985), "Hydrodynamics of Fluidization: Prediction of Wall to Bed Heat Transfer Coefficients", *AIChE J*, **31**, No.1, 127-135.

SYAMLAL, M., and O'BRIEN, T.J. (1988), "Simulation of Granular Layer Inversion in Liquid Fluidized Beds", *Int. J. Multiphase Flow*, **14**, No. 4, 473-481.

TANAKA, M., MAZUMDAR, D. and GUTHRIE, R.I.L. (1993), "Motions of Alloying Additions During Furnace Tapping in Steelmaking Processing Operations", *Met. Trans. B*, **24B**, 639-648.

VAN LEER, B. (1974), "Towards the Ultimate Conservative Difference Scheme. II Monotonicity and Conservation Combined in a Second-Order Scheme", *J. Comp. Phys.*, **14**, 361-370.

WRIGHT, J.K., and BALDOCK, B.R. (1988), "Dissolution Kinetics of Particulate Graphite injected into Iron/Carbon Melts", *Met. Trans. B*, **19B**, 375-382.